Threshold Analysis of Pulsed Lasers with Application to a Room-Temperature $Co:MgF_2$ Laser

JAMES HARRISON, DAVID WELFORD, MEMBER, IEEE, AND PETER F. MOULTON, SENIOR MEMBER, IEEE

Abstract—**Rate-equation calculations have been used to accurately model the near-threshold behavior of a $Co:MgF_2$ laser operating at room temperature. The results demonstrate the limitations of the conventional threshold analysis in cases of practical interest. This conclusion is applicable to pulsed solid-state lasers in general. The calculations, together with experimental data, have been used to determine emission cross sections for the $Co:MgF_2$ laser.**

Introduction

$Co:MgF_2$ is a tunable solid-state laser material of great interest for applications including remote sensing and clinical medicine. At room temperature the $Co:MgF_2$ laser operates over the 1750–2500 nm range. As part of an ongoing development program, a normal-mode $Co:MgF_2$ laser, longitudinally pumped by a Nd:YAG laser operating at 1.338 μm, has been studied experimentally and theoretically over a wide range of operating temperatures and pump conditions. The results indicate that the temporal behavior can be accurately modeled with rate-equation calculations [1]. However, it has not been possible to accurately predict the absolute input/output characteristics. This is due to the fact that the threshold analysis [2] that is conventionally applied to such systems neglects the effect of photons stored in the cavity during the prelase period (i.e., the "cavity build-up time interval"). It is the purpose of this paper to demonstrate their importance in cases of practical interest. Accurate modeling requires consideration of both the upper-state lifetime τ and the cavity lifetime τ_c in numerical rate-equation analyses. While this result is particularly important for the room-temperature $Co:MgF_2$ laser [3], it should be considered generally applicable to the analysis of pulsed, laser-pumped solid-state lasers including $Ti:Al_2O_3$ [4] and diode-pumped rare-earth devices.

In situations where the pump-pulse duration is very short compared to the upper-state lifetime ($\tau_p \ll \tau$), build-up time effects are typically ignored because spontaneous emission losses are negligible. However, recently Eggleston *et al.* [4] have demonstrated that the nonzero build-up time interval can have a strong influence on the behavior of gain-switched $Ti:Al_2O_3$ lasers near threshold.

Manuscript received October 28, 1988; revised January 29, 1989. This work was supported by NASA under Contract NAS1-18442 of the Small Business Innovative Research Program.

The authors are with Schwartz Electro-Optics, Concord, MA 01742.

IEEE Log Number 8928002.

The normal-mode $Co:MgF_2$ laser is often operated in an intermediate regime in which the pump-pulse duration is comparable to the upper-state lifetime ($\tau_p \sim \tau$). In this case, these effects are evident well beyond threshold.

In his investigation of the $Co:MgF_2$ laser, Moulton [2] extended previous work [5], [6] to derive the following expression for the CW threshold of a longitudinally pumped laser:

$$P_p(\text{th}) = (\pi h\nu_p w_L^2/4\sigma\tau)(L + T)(a^2 + 1) \cdot \left[1 - \exp(-\alpha l_g)\right]^{-1} \quad (1)$$

where $P_p(\text{th})$ is the pump power incident on the gain medium at threshold, $h\nu_p$ is the pump photon energy, w_L is the laser mode spot size in the gain medium of length l_g, σ is the emission cross-section of the laser transition, L is the internal cavity loss per roundtrip, T is the output coupling loss, and α is the absorption coefficient at the pump wavelength. The mode overlap parameter $a = (w_p/w_L)$ is the ratio of the pump spot size to that of the cavity mode. For lasers involving a Brewster-cut laser crystal, the above expression for $P_p(\text{th})$ should be multiplied by the index of refraction of the crystal to account for astigmatism. Assuming a constant-power pump pulse, the pulsed threshold $E_p(\text{th})$ is given by [2]

$$E_p(\text{th}) = P_p(\text{th})\,\tau_p\left[1 - \exp(-\tau_p/\tau)\right]^{-1}. \quad (2)$$

Note that in (1) and (2) the cavity losses have essentially been decoupled from the spontaneous losses. Equation (1) is the familiar statement that gain equals loss at threshold. Equation (2) accounts for spontaneous emission with the assumption that the build-up time interval at threshold is equal to the pump-pulse duration. The gain medium is treated as a simple integrator of pump energy. Equation (2) does not account for the fact that the laser cavity provides a reservoir of photons with a capacity that increases with the cavity lifetime. This stored field may allow the build-up time interval at threshold to significantly exceed the pump-pulse duration. In such a case, (2) will yield an unrealistically low threshold due to the underestimate of the spontaneous loss. The significance of the error depends strongly on the absolute value of the cavity lifetime and the relative values of the pump-pulse duration τ_p and the upper-state lifetime τ. Thus, the major source of error in estimating the laser threshold arises from inaccurate predictions of the spontaneous emission loss during the build-up time interval.

This issue is particularly relevant to the analysis of the room-temperature $Co:MgF_2$ laser [3]. The upper-state lifetime rapidly decreases from $\tau = 1.2$ ms at 77 K to $\tau = 36.5$ μs at 300 K [2]. In order to obtain efficiencies similar to those demonstrated at cryogenic temperatures, the room-temperature laser must be driven by a rapidly rising pump pulse so that a quasi-CW inversion is established in a time short compared to the upper-state lifetime. In normal mode operation, the pump-pulse duration is typically tens to hundreds of microseconds in duration. Hence, the pump-pulse duration is longer than the upper-state lifetime ($\tau_p > \tau$) for room-temperature operation and accurate modeling requires some numerical analysis beyond (1) and (2).

The temporal characteristics, threshold behavior and input/output curves for normal-mode laser operation may be described by a pair of coupled rate equations relating the spatially averaged population inversion density N and photon density, ϕ. The effects of nonuniform absorption of pump-laser radiation and the corresponding distributions of the inversion and photon densities are omitted from this analysis. The rate equations are as follows:

$$\frac{d\phi}{dt} = \frac{c\sigma l_g N\phi}{l_c} - \frac{\phi}{\tau_c} + W_n \tag{3}$$

and

$$\frac{dN}{dt} = W_p - \frac{N}{\tau} - \frac{c\sigma l_g N\phi}{l_c} \tag{4}$$

where c is the speed of light, l_c is the cavity length, σ is the emission cross section, l_g is the length of the gain medium, and τ_c is the cavity lifetime. W_n and W_p are the photon generation terms for blackbody and spontaneous emission, and for the pump laser, respectively. The rate-equations were normalized in the manner described by Wagner and Langyel [1] and evaluated numerically using a Runge–Kutta algorithm.

Rate-equation simulations [using (3) and (4)] assuming rectangular pump pulses clearly indicate the limitations of the conventional threshold model. Fig. 1 shows the calculated output energy, on a logarithmic scale, as a function of input energy for a room-temperature $Co:MgF_2$ laser. Threshold is defined as the input energy at the intersection between two linear fits to the data: one applied well below threshold and one applied well above threshold. The pump pulse was assumed to be 300 μs in duration at constant power. To correspond closely to measured experimental parameters, the laser cavity was assumed to be 49 cm long with $L = 0.5$ percent. Numerical results are included for three output couplers with reflectivities of $R = \{95, 98, 99.5 \text{ percent}\}$. The corresponding cavity lifetimes are $t_c = \{58, 130, \text{and } 326 \text{ ns}\}$. The abscissa of Fig. 1 has been normalized, for $R = 99.5$ percent, to the threshold determined by (1) and (2) which predict relative thresholds for the three cases of 5.5, 2.5, and 1.0, respectively. In order to accurately normalize the calculations, a quasi-CW simulation was performed ($\tau_p = 10$ ms, $\tau = 36.5$ μs, $E_p(\text{th}) = P_p(\text{th})\,\tau_p$). In this case, the build-up time interval never exceeded the pump pulse

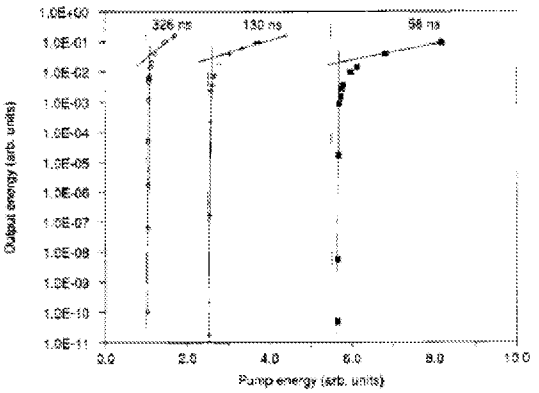

Fig. 1. Calculated input/output curves showing threshold behavior for a 300 μs duration pump pulse. The three curves are for cavity lifetimes of 58, 130, and 326 ns. The dashed vertical lines represent the thresholds determined by (1) and (2).

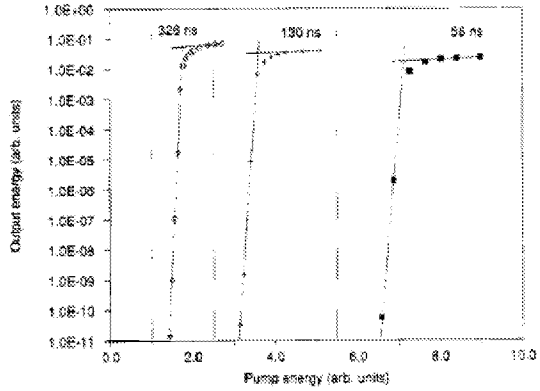

Fig. 2. Calculated input/output curves showing threshold behavior for a 30 μs duration pump pulse. The three curves are for cavity lifetimes of 58, 130, and 326 ns. The dashed vertical lines represent the thresholds determined by (1) and (2).

duration and the calculated thresholds were related by the 5.5 : 2.5 : 1.0 ratio predicted by (1) and (2).

Similar numerical results are included in Figs. 2 and 3 for 30 and 3 μs rectangular pump pulses, respectively. In both figures, the abscissa has been normalized as in Fig. 1 (i.e., in absolute terms, the input-energy units of Figs. 2 and 3 are $0.18x$ and $0.13x$ those of Fig. 1, respectively).

Figs. 1–3 clearly indicate the importance of augmenting (1) and (2) with rate-equation calculations. This is especially true when the pump-pulse duration is shorter than the upper-state lifetime ($\tau_p < \tau$), in which case the correction to threshold increases with the photon lifetime of the cavity τ_c. These results suggest a simple correction to (2):

$$E_p(\text{th}) = P_p(\text{th})\,\tau_d\left[1 - \exp\left(-\tau_d/\tau\right)\right]^{-1} \tag{5}$$

where the build-up time interval at threshold, τ_d, is substituted for pump-pulse duration, τ_p. Table I compares the results of the rate-equation calculations to those of (2) and (5) for $\tau = 36.5$ μs. In (5), the build-up time interval τ_d was taken as the delay between the onset of the pump pulse and the peak of the $Co:MgF_2$-laser pulse at threshold. It is apparent from the table that (5) is not sufficiently accurate to obviate the rate-equation analysis.

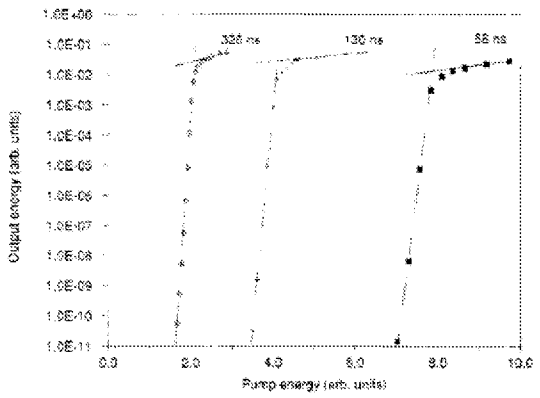

Fig. 3. Calculated input/output curves showing threshold behavior for a 3 μs duration pump pulse. The three curves are for cavity lifetimes of 58, 130, and 326 ns. The dashed vertical lines represent the thresholds determined by (1) and (2).

TABLE I
CALCULATED THRESHOLD ENERGIES, IN NORMALIZED UNITS, FOR THE Co:MgF_2 LASER AT ROOM TEMPERATURE

τ_p (μsec)	τ_c (nsec)	τ_d (μsec)	Threshold Energy (Eqs. 1-2)	Threshold Energy (Eqs. 1,3)	Threshold Energy (Rate Eqs.)
3	326	27.9	1.00	1.36	2.67
3	130	15.9	2.50	2.86	4.69
3	58	12.6	5.50	6.24	7.84
30	326	47.3	1.41	1.71	2.50
30	130	35.9	3.52	3.77	5.36
30	58	32.6	7.74	8.09	10.7
300	326	300	7.89	7.89	8.75
300	130	300	19.7	19.7	21.5
300	58	300	42.7	42.7	50.6

Fig. 4 extends the calculations of Fig. 2 (τ_p = 30 μs, R = 98 percent) to well above threshold. The results, shown on a linear scale, demonstrate detailed behavior common to many normal-mode lasers [4]. The undulations in the output energy near threshold correspond to integral increases in the number of discrete output pulses generated per pump pulse. The characteristic appears linear only when quasi-CW operation is achieved.

Actual laser experiments (R = 98 percent, 2.100 μm) were modeled numerically with digitized pump-pulse profiles. Fig. 5 shows the digitized pump pulse, the output pulse calculated with the rate equations, and the corresponding experimental oscilloscope photographs for operation of a room temperature Co:MgF_2 laser [3] at approximately 2.5x threshold. The agreement between the experimental data and the numerical results in Fig. 5(b) demonstrate the accuracy of the rate-equation model. In particular, the build-up time interval τ_d and the temporal form of the output are sensitive indicators of the accuracy of the rate-equation model. Close agreement between experimental data and numerical simulations requires digitization of the actual pump-pulse profile at each experimental pump energy. Fig. 6 shows both experimental and numerical input/output curves that show excellent agreement for pump energies up to 4x threshold. The deviation

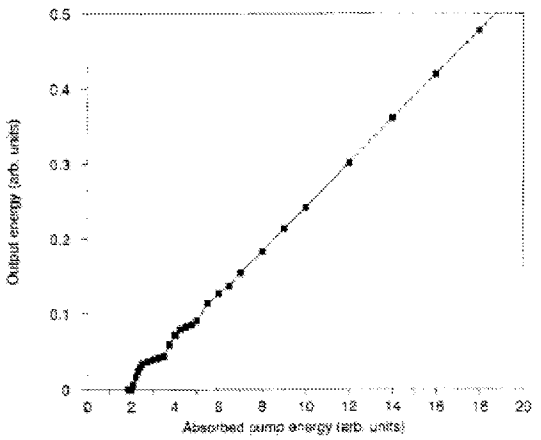

Fig. 4. Calculated input/output curve for a 30 μs duration pump pulse, 130 ns cavity lifetime, and 36.5 μs upper-state lifetime, extended to well above threshold.

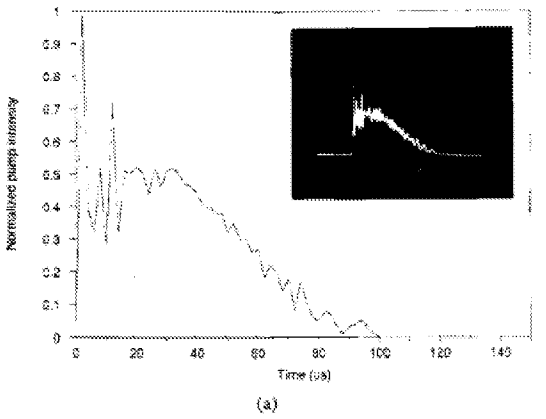

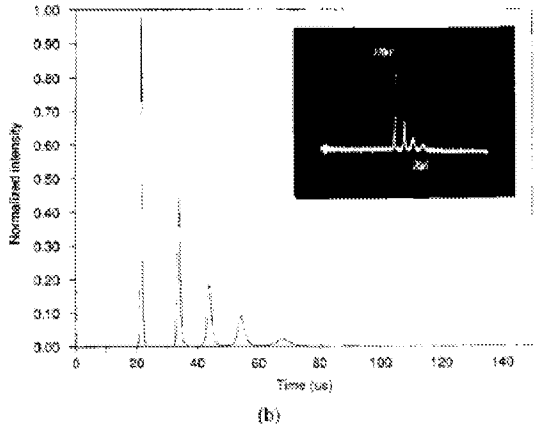

Fig. 5. (a) Digitized and measured experimental pump pulse for a room temperature Co:MgF_2 laser at 2.5x threshold. (b) Rate-equation and measured output pulses for a room temperature Co:MgF_2 laser at 2.5x threshold. The inset photographs show a total timespan of 200 μs.

from linearity at higher pump energies is due to thermal lensing of the pump laser. This was confirmed by measuring the spot size of the focused pump-beam at the laser crystal as a function of pump energy. Thermal lensing increases the divergence of the Nd:YAG beam thereby reducing the coupling between the pump and the

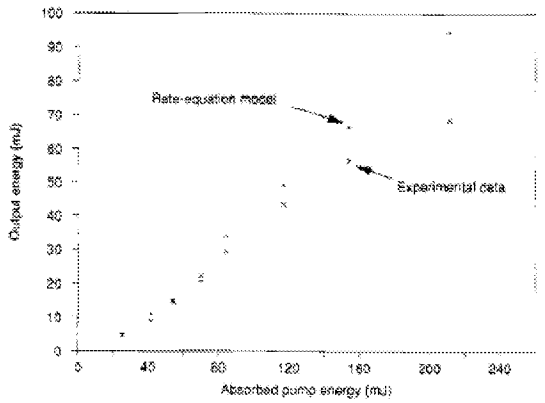

Fig. 6. Comparison of calculated and experimental input/output data for a $Co:MgF_2$ laser operating at room temperature.

TABLE II
PEAK EMISSION CROSS SECTIONS, AND CORRESPONDING WAVELENGTHS, FOR THE $Co:MgF_2$ LASER AT THREE OPERATING TEMPERATURES. THE PARAMETERS σ_π AND σ_σ REFER TO THE CROSS SECTIONS FOR POLARIZATION PARALLEL AND PERPENDICULAR TO THE c-AXIS OF THE $Co:MgF_2$ CRYSTAL, RESPECTIVELY

Temperature (K)	*Wavelength (μm)*	σ_π $(10^{-20}\ cm^2)$	σ_σ $(10^{-20}\ cm^2)$
248	2.318	4.5	
248	2.009		9.7
279	2.326	4.8	
279	2.116		11
299	2.330	4.6	
299	2.130		9.3

$Co:MgF_2$ laser [this corresponds to an increase in the overlap parameter a in (1)].

Given the agreement between the experimental data and the rate-equation model for both temporal behavior and input/output characteristics, we have used the threshold analysis, along with measured threshold energies, to determine peak emission cross sections as functions of wavelength and temperature. Emission cross sections are listed in Table II along with the wavelengths of the gain peaks for 248, 279, and 299 K.

In summary, the general analysis of (2) may not yield useful estimates for laser thresholds in situations of practical interest. Rate-equation calculations, used to supplement (2) do yield accurate simulations. The range of calculations included here demonstrate the degree of correction for several important regimes of laser operation. These results are generally applicable to pulsed, laser-pumped solid state lasers. Finally, experimental data obtained with a $Co:MgF_2$ laser are shown to be in excellent agreement with the numerical results. With the ability to accurately model the laser, it has been possible to determine peak emission cross sections for the $Co:MgF_2$ laser at three operating temperatures.

REFERENCES

[1] W. G. Wagner and B. A. Lengyel, "Evolution of the giant pulse in a laser," *J. Appl. Phys.*, vol. 34, pp. 2040–2046, 1963.
[2] P. F. Moulton, "An investigation of the $Co:MgF_2$ laser system," *IEEE J. Quantum Electron.*, vol. QE-21, pp. 1582–1595, 1985.
[3] D. Welford and P. F. Moulton, "Room-temperature operation of the $Co:MgF_2$ laser," *Optics. Lett.*, vol. 13, pp. 975–977, 1988.
[4] J. M. Eggleston, L. G. DeShazer, and K. W. Kangas, "Characteristics and kinetics of laser-pumped Ti:Sapphire oscillators," *IEEE J. Quantum Electron.*, vol. 24, pp. 1009–1015, 1988.
[5] L. W. Casperson, "Laser power calculations: sources of error," *Appl. Opt.*, vol. 19, pp. 422–434, 1980.
[6] D. G. Hall, R. H. Smith, and R. R. Rice, "Pump-size effects in Nd:YAG lasers," *Appl. Opt.*, vol. 19, pp. 3041–3043, 1980.

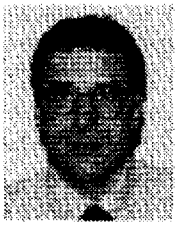

James Harrison was born in New Haven, CT, on May 31, 1956. He received the B.S., M.S., E.E., and Ph.D. degrees from the Department of Electrical Engineering and Computer Science, Massachusetts Institute of Technology, Cambridge, where he was awarded the N.C.R. Fellowship for 1985–1986. His doctoral dissertation, completed in 1986, involved a study of the spectral properties of semiconductor diode lasers and included the development of ultrastable external cavity lasers. This work was performed in the Quantum Electronics Group at M.I.T. Lincoln Laboratory, Lexington.

From 1981 to 1982 he was an Electronics Engineer in the Laser Isotope Separation Program at Lawrence Livermore National Laboratory, Livermore, CA. There he worked on the development of the dye master oscillator and performed a spectroscopic study of the source metal vapor. In 1985 he was a summer staff member at M.I.T. L.L. Since 1987 he has been at Schwartz Electro-Optics, Research Division, Concord, MA. His work focuses on the development of single-frequency solid-state lasers. These include both pulsed and CW diode-pumped systems, and involve a variety of materials for visible, near-infrared, and eye-safe applications.

Dr. Harrison is a member of the Optical Society of America and Sigma Xi.

David Welford (S'79–M'80) was born in Whitby, North Yorkshire, England, on March 17, 1956. He received the B.Sc. degree in 1977, and the Ph.D. and D.I.C. degrees in 1980, all in physics, from the Imperial College of Science and Technology, University of London, England. His thesis research was on CW mode-locked dye lasers and their application in picosecond kinetics studies of organic molecules.

He was with the Massachusetts Institute of Technology Lincoln Laboratory, Lexington, MA, from 1980 to 1987, where he investigated the emission linewidth and modulation properties of semiconductor diode lasers and the application of diode lasers to optical communications. Since April 1987 he has been with Schwartz Electro-Optics Inc., Concord, MA. His primary research interests are tunable solid state laser materials and semiconductor diode pumped lasers.

Dr. Welford is a member of the Optical Society of America.

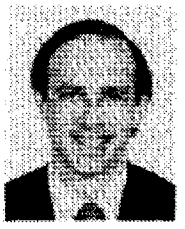

Peter F. Moulton (M'69–S'74–SM'84) was born in Springfield, MA, on May 27, 1946. He received the A.B. degree in physics from Harvard College, Cambridge, MA, in 1968 and the M.S. and Ph.D. degrees from the Department of Electrical Engineering and Computer Science, Massachusetts Institute of Technology, Cambridge, in 1971 and 1975, respectively.

He spent a postdoctorate year in 1975 at M.I.T. Lincoln Laboratory, Lexington, and became a Staff Member there in 1976. His work at Lincoln Laboratory included high-resolution infrared spectroscopic measurements of molecules, development of lasers or remote sensing, and research and development of tunable and high-efficiency solid state lasers. Since 1985 he has been Vice President and General Manager of the Research Division of Schwartz Electro-Optics, Concord, MA, where he is engaged in the research and development of a new solid-state laser materials and systems.

Dr. Moulton is a member of the Optical Society of America and Sigma Xi.